Author Manuscript

Author Manuscript

Author Manuscript

Author Manuscript

HHS Public Access

Author manuscript

IEEE Trans Biomed Eng. Author manuscript; available in PMC 2017 October 01.

Published in final edited form as:

IEEE Trans Biomed Eng. 2017 October ; 64(10): 2353–2360. doi:10.1109/TBME.2016.2641958.

Wearable Vector Electrical Bioimpedance System to Assess Knee Joint Health

Sinan Hersek,
School of Electrical and Computer Engineering (ECE), Georgia Institute of Technology, Atlanta, GA 30308 USA

Hakan Töreyin [Member, IEEE],
School of Electrical and Computer Engineering (ECE), Georgia Institute of Technology, Atlanta, GA 30308 USA

Caitlin N. Teague [Student Member, IEEE],
School of Electrical and Computer Engineering (ECE), Georgia Institute of Technology, Atlanta, GA 30308 USA

Mindy L. Millard-Stafford,
School of Biological Sciences, Georgia Institute of Technology, Atlanta, GA 30308 USA

Hyeon-Ki Jeong,
School of Electrical and Computer Engineering (ECE), Georgia Institute of Technology, Atlanta, GA 30308 USA

Miheer M. Bavare,
School of Electrical and Computer Engineering (ECE), Georgia Institute of Technology, Atlanta, GA 30308 USA

Paul Wolkoff,
Georgia Tech Athletic Association, Atlanta, GA

Michael N. Sawka, and
School of Biological Sciences, Georgia Institute of Technology, Atlanta, GA 30308 USA

Omer T. Inan [Senior Member, IEEE]
School of ECE and, as an adjunct, the Coulter Department of Biomedical Engineering, Georgia Institute of Technology, Atlanta, GA 30308 USA

Abstract

Objective—We designed and validated a portable electrical bioimpedance (EBI) system to quantify knee joint health.

Methods—Five separate experiments were performed to demonstrate the: (1) ability of the EBI system to assess knee injury and recovery; (2) inter-day variability of knee EBI measurements; (3) sensitivity of the system to small changes in interstitial fluid volume; (4) reducing the error of EBI

inan@gatech.edu, ph: 404-385-1724.

Author Manuscript Author Manuscript Author Manuscript Author Manuscript

measurements using acceleration signals; (5) use of the system with dry electrodes integrated to a wearable knee wrap.

Results—(1) The absolute difference in resistance (R) and reactance (X) from the left to the right knee was able to distinguish injured and healthy knees ($p<0.05$); the absolute difference in R decreased significantly ($p<0.05$) in injured subjects following rehabilitation. (2) The average inter-day variability (standard deviation) of the absolute difference in knee R was 2.5Ω, and for X was, 1.2 Ω. (3) Local heating/cooling resulted in a significant decrease/increase in knee R ($p<0.01$). (4) The proposed subject position detection algorithm achieved 97.4% leave-one subject out cross-validated accuracy and 98.2% precision in detecting when the subject is in the correct position to take measurements. (5) Linear regression between the knee R and X measured using the wet electrodes and the designed wearable knee wrap were highly correlated ($r^2 = 0.8$ and 0.9, respectively).

Conclusion—This work demonstrates the use of wearable EBI measurements in monitoring knee joint health.

Significance—The proposed wearable system has the potential for assessing knee joint health outside the clinic/lab and help guide rehabilitation.

Index Terms

Electrical bioimpedance; joint physiology; wearable sensing

I. Introduction

Electrical bioimpedance (EBI) is a technique that involves passing a small amount of electrical current through a volume of biological tissue, and measuring the ensuing voltage change across that tissue to calculate the passive impedance imposed against electrical current flow [1]. Because the electrical conductivity for different types of tissue varies significantly, such EBI measures can provide information regarding the underlying structural composition of the tissue volume [2].

EBI is often measured at a single frequency of excitation—typically in the tens of kHz or higher to reduce losses due to the skin-electrode interface and also allow for higher safety limits on current levels of excitation—but can also be measured at multiple frequencies to allow for bioimpedance spectroscopy [3]. Applications of the method have included the use of EBI for body composition analysis (i.e., estimation of fat-free mass and total body water) [4, 5], blood volume pulse and limb blood flow quantification [6, 7], cardiac output and function [8, 9], detection of cardiac events such as aortic valve opening [10], wound healing monitoring [11], and, recently, muscle injury and edema assessment [12–14]. To our knowledge, evaluation of EBI as a tool for quantifying knee joint health following acute knee injuries – which may be more subtle as compared to total knee replacement surgery as previously considered [14] – has not been examined by others in the existing literature. Additionally, these previous approaches were mainly limited to controlled lab settings, using bench-top, wall-powered equipment, which are not applicable in a wearable setting.

Author Manuscript Author Manuscript Author Manuscript Author Manuscript

Recently, our group presented a novel proof-of-concept system for vector EBI measurements that could potentially be used for quantifying knee joint health following an acute injury, in a wearable setting [15]. We presented results from a small preliminary dataset of 9 subjects (7 healthy, and 2 with injured knees) in that previous paper, and showed promising initial results comparing the impedance characteristics of the injured versus healthy leg: the differences between legs in resistance and reactance were greater for the subjects with recently acquired acute injury as compared to the healthy subjects.

In this paper, we present a comprehensive validation of our methods, and unlike previous approaches ([12–14]), we demonstrate engineering contributions which can facilitate translating our technique from the lab to the field or home, including: (1) a larger study on 49 subjects (42 healthy, 7 injured) to validate the performance of the technology in quantifying physiological differences in the knee; (2) a study of the inter-day measurement variability to determine the minimum bioimpedance change that can, with confidence, be attributed to edema as compared to measurement error; (3) a physiological perturbation study aimed at creating small changes in local interstitial fluid volume in the knee based on modulating tissue temperature to quantify the sensitivity of the vector EBI system; (4) an algorithm for automatically detecting periods of high reliability, for gating the data acquisition; and (5) evaluation of a wearable knee wrap-based implementation of our system, with copper band electrodes.

II. System Design and Methods

A. Bioimpedance Measurement System

A custom analog front-end is used to acquire static and dynamic bioimpedance measurements from the knee joint. Note that, in this work, “static” bioimpedance is considered the slowly varying component of impedance that would change based on structural modifications of the tissue volume (i.e., edema); “dynamic” bioimpedance, on the other hand, captures the mΩ level fluctuations in the tissue impedance that are cardio-synchronous, and associated with the blood volume pulse. The block diagram of the measurement setup is shown in Fig. 1 (a).

A sinusoidal current is input to the knee (frequency 50 kHz, and amplitude 2 mA_{pp}) via electrodes E1 and E4; the voltage drop resulting from this current excitation is detected from electrodes E2 and E3. The circuit also senses the delivered current to subsequently correct for any variability over time ($v_{sense}(t)$). An I/Q demodulator consisting of in-phase ($i(t)$) and quadrature ($q(t)$) phase sensitive detection and filtering is used to find both in-phase and quadrature components of the measured voltage. The signal ($v_{sense}(t)$) is passed through amplitude detection to get the signal $A(t)$ which is used to monitor the amplitude of the injected current.

The signals are then recorded using an MP150 data acquisition system (Biopac Systems Inc., Goleta, CA) with a sampling rate of 2 kHz. The amplitude correction (compensating for any variations in current amplitude during the measurement) and calibration (converting the voltage signals $i(t)$ and $q(t)$ into impedance signals) steps are carried out in post-processing using MATLAB (Mathworks, Natick, MA). For more details regarding the circuit and

Author Manuscript Author Manuscript Author Manuscript Author Manuscript

system design details, as well as the algorithms used for calibration and amplitude correction, the reader is referred to [15].

B. Position Identification Algorithm

Bioimpedance measurements are greatly impacted by motion artifacts and subject position [16–18]. Our ultimate goal is to design a wearable system that can be used outside of laboratory/clinical settings, and thus must be "smart" in that it can automatically identify times at which the body position is such that robust, and consistent, EBI measurements can be obtained. We developed an algorithm that can detect such instants in time based on signals from two dual axis accelerometers, placed laterally on the thigh and shank (Fig. 1(b)). The EBI signals are then gated by determining instances where the subject is still and in a certain position, using information obtained from the accelerometers.

We have used the signals from the dual axis accelerometers placed on the thigh ($\boldsymbol{a_{th}(t)} = [a_{th,x}(t)\ a_{th,y}(t)]^T$) and the shank ($\boldsymbol{a_{sh}(t)} = [a_{sh,x}(t)\ a_{sh,y}(t)]^T$) to determine a consistent body position for measurement: seated posture with legs fully extended and supported. This position is preferred for EBI measurements as it provides a completely unloaded and easily repeatable position, which will reduce artifacts and variability in measurements. The position identification algorithm is summarized in Fig. 1(c) and includes windowing (10 sec windows, 50% overlap), feature extraction, and binary classification. Features extracted from each ten second frame are used to label the frame as reject (0) meaning the subject is not in the desirable position described above or accept (1). The labels for these frames are then used to determine which resistance/reactance measurements can be assumed as robust and thus stable.

The binary decision rule mentioned is trained separately before it is applied to new data (a testing set). For this training, the signals from the two accelerometers are recorded from multiple subjects (six in our case), while the subject performs the following activities with known labels: (1) standing (label 0), (2) sitting legs bent (label 0), (3) sitting legs crossed (label 0), (4) sitting legs extended and supported (label 1) and (5) walking (label 0) each for 1 minute. The subjects perform a combination of the listed activities for 13 minutes, where for approximately three minutes, the subject is sitting with legs extended and supported. Feature extraction is performed on the accelerometer signals from the six subjects as shown on Fig. 1(c) to produce a feature vector $\boldsymbol{F_{training}}$ and the corresponding known labels $\boldsymbol{d_{training}}$.

Exhaustive grid search with leave-one-subject-out (LOSO) cross-validation is used to determine the set of hyper-parameters and kernel to be selected for the support vector machine (SVM) classifier to be trained [19, 20]. The kernels considered in the search are linear and radial basis function (RBF) kernels. The set of values considered for the hyper-parameter C are numbers logarithmically spaced between 10^{-2} and 10^{3} for both kernels. The γ parameter for the RBF kernel is chosen from the set $\{10^{-4}, 10^{-3}, 10^{-2}\}$. A kernel and a value for C (and γ if the RBF kernel is selected) is chosen and the LOSO cross-validation accuracy score of the model is computed using $\boldsymbol{F_{training}}$ and $\boldsymbol{d_{training}}$. The same procedure is repeated for all combinations of kernels, C values and γ values (for models where the kernel is RBF). The model that maximizes the LOSO cross-validation accuracy within the models

Author Manuscript Author Manuscript Author Manuscript Author Manuscript

included in the search is selected. Finally an SVM classifier with the selected kernel and hyper-parameter(s) is trained on $\boldsymbol{F}_{training}$ and $\boldsymbol{d}_{training}$ resulting in the binary decision rule to be used. The training and model selection is done once and is expected to generalize well for new subjects. SVM was chosen as a classification algorithm as it provides many degrees of freedom in model selection by allowing the use of various kernels and multiple hyper-parameters (C and γ). An exhaustive grid-search is used to be able to select the one that will generalize the best, from the set that is considered. The model selection and SVM training steps are carried out using the Scikit-learn library for the Python programming language.

The features extracted for each frame are the mean and the standard deviation of each of the four accelerometer signals ($a_{th,x}(t)$, $a_{th,y}(t)$, $a_{sh,x}(t)$, $a_{sh,y}(t)$) resulting in eight features per frame. The feature extraction stage was performed in MATLAB.

C. Human Subject Studies and Measurement Protocols

Five separate human subject studies were conducted to assess the bioimpedance measurement system and the designed algorithm. All human subject studies were approved by the Georgia Institute of Technology Institutional Review Board (IRB) and the Army Human Research Protection Office (AHRPO).

1) Discriminating Healthy versus Injured Knees and Monitoring Longitudinal Injury Recovery—In the first test performed, the bioimpedance measurement system was used to acquire measurements from 49 subjects. Out of these subjects, 42 were healthy, control subjects (27 male, 15 female) with no history of recent injury to any knee. Seven subjects (six male, one female) had a recent acute, unilateral knee injury (within one month before the measurement date), requiring subsequent corrective surgery (torn anterior cruciate or medial collateral ligament, and/or lateral meniscus). All injured subjects and 36 of the control subjects were college athletes.

Standard wet gel (Ag/AgCl) adhesive backed electrodes (2660-3 Red dot electrodes, 3M, Maplewood, MN) were positioned on the subjects' legs as shown in Fig. 4(a). The proximal current electrode (E1) was placed three inches above the crease on the quadriceps tendon, towards the medial side of the knee. The distal current electrode (E4) was placed three inches below the popliteal fossa, towards the lateral side of the knee. The voltage electrodes (E2, E3) were placed adjacent to the current electrodes [15]. Subjects were asked to sit with their back against the wall, legs extended forward. While the subject sat still (to rule out motion artifacts), the signals were recorded on a laptop using the MP150 data acquisition system. Measurements were taken from both knees of each subject. Later, the in-phase and quadrature signals were amplitude corrected and calibrated to get the static resistance and reactance signals. The mean of these signals over 60 seconds was taken to compute knee resistance and reactance of a given subject. This protocol was repeated on the seven injured subjects, on one occasion several months (4–7) after corrective surgery was performed.

2) Day-to-Day Variability in EBI Measurements—A second test was performed to investigate the day-to-day variability of the knee impedance measures. EBI measurements were acquired from five healthy subjects for three days within a week under standard conditions (e.g., no previous exercise and same time of day). The electrodes and electrode

Author Manuscript Author Manuscript Author Manuscript Author Manuscript

configuration in the first test were used and measurements were taken from both knees. Since the first human study indicated that the difference in resistance from left to right knee was an important parameter for separating healthy from injured knees, the day-to-day variability in this parameter in particular was quantified.

3) Investigating Effects of Local Heating/Cooling on EBI—A third test was performed for seven healthy subjects to investigate the effects of local tissue heating and cooling on knee bioimpedance. Tissue (skin and muscle) heating will decrease pre- to post-capillary resistance ratios thus resulting in net capillary filtration and increasing interstitial fluid, while local cooling will have the opposite effect [21]. In this test, the subject's knee bioimpedance was recorded (with the same electrodes, electrode placement and subject positioning as the first test) while the knee was locally cooled using a standard ice-pack (Pro-Tec Athletics, Richmond WA) on the anterior patella for 20 minutes. Skin temperature on the patella was measured using a resistance temperature detector (SA2CRTD-3-1000-A, Omega Engineering, Stamford, CT). The temperature was logged using a data logger (HH126, Omega Engineering, Stamford, CT) with a sampling rate of 1 Hz. After waiting for the skin temperature to return to its baseline value, the test was repeated with a hot pack (Chattanooga Medical Supply Inc., Chattanooga, TN).

4) Optimal Position Identification Algorithm—Experiments were performed on seven healthy subjects to evaluate the position identification algorithm. Dual axis accelerometers (ADXL203EB, Analog Devices, Norwood, MA) were placed on the subjects' right leg as shown on Fig. 4(a). The accelerometer on the thigh was placed six inches above the crease on the quadriceps tendon on the lateral side of the knee. The accelerometer on the shank was placed six inches below the crease on the popliteal fossa at the lateral side of the knee as well. The accelerometers were held in place using athletic tape. The electrodes and electrode configuration used were the same as in the first experiment. The accelerometer and EBI signals were recorded from each subject while the subject performed the five activities mentioned in Section II.B, for one minute each. The signals from the EBI analog front-end and the accelerometers were acquired using the MP150 data acquisition system and were recorded on a laptop. A combination of these activities was performed for 13 minutes.

LOSO cross-validation was performed to assess the performance of the position identification algorithm described in Section II.B. In each fold of the cross-validation, a binary classifier was trained on all subjects except the one that was left out in that particular fold. The model was tested on the subject that was left out of training, and the accuracy and precision were calculated. The resistance and reactance signals for the testing subject were gated using the predicted labels such that the frames labeled "1" are kept and the rest are removed. The variability of the resistance and reactance signals across frames were computed both when gating is performed and not performed. This comparison is done to demonstrate how gating reduces measurement variability and increases consistency. The train-test procedure was repeated for all subjects and the accuracy, precision and variability metrics were averaged across the LOSO cross-validation folds.

5) Evaluation of a Knee Wrap with Dry Electrodes Integrated—Experiments were performed on seven control subjects to demonstrate the usability of the bioimpedance

Author Manuscript Author Manuscript Author Manuscript Author Manuscript

measurement system with dry electrodes integrated into a knee brace. For this test, bioimpedance signals were acquired from a subject using Ag/AgCl wet gel electrodes, with the aforementioned electrode configuration and while the subject was seated, with legs extended and supported from the bottom, for 60 seconds. Then the subject was asked to wear the designed brace shown in Fig. 5(a) to (c). The brace consists of two wraps, each containing the proximal (E1 and E2) and distal (E3 and E4) electrodes. Each electrode consists of five 1.6 inch by 1.2 inch rectangles cut out of plastic and covered with copper tape, that are electrically shorted to each other. The brace was positioned such that the electrodes were at similar positions to the ones in the prior tests as shown on Fig. 5 (a) and (b). Signals were acquired while the subject was still, in the same position for 60 seconds. The signals were amplitude corrected and calibrated to get the resistance and reactance signals measured using wet and dry electrodes. The measured resistance and reactance which was compared for wet and dry electrodes, was calculated by averaging the resistance and reactance signals over the 60 second time interval.

III. Results and Discussion

A. Physiological Measurements

1) Discriminating Healthy versus Injured Knees and Monitoring Longitudinal Injury Recovery—The bioimpedance measurement results obtained for the first study are shown on Fig. 2(a). The difference in resistance between the knees for the healthy subjects (left minus right) was 1.9 ± 5.6 Ω. The difference in reactance was −1.1 ± 2.4 Ω. The difference in resistance between the knees (injured side minus healthy side) for the injured subjects was −11.8 ± 4.5 Ω. The difference in reactance was 4.9 ± 2.6 Ω. The absolute differences in resistance between the knees for the healthy subjects (left vs. right knee) were 4.9 ± 3.3 Ω while for injured subjects were 11.8 ± 4.6 Ω ($p<0.05$, two sample t-test with unknown and unequal variances). Similarly, the absolute difference in reactance between the knees were 2.2 ± 1.4 Ω for the healthy subjects and 4.9 ± 2.6 Ω for the injured subjects ($p<0.05$, two sample t-test with unknown and unequal variances).

For all of the injured subjects, the affected knee had lower resistance than the healthy one. For all but one injured subject, the affected side had a higher reactance (lower negative reactance) than the healthy one; the one outlier injured subject had almost no difference (0.02 Ω) in reactance between the knees.

The effect of injury recovery on the difference in impedance between the knees is shown on Fig. 2(b). The difference in resistance between the knees for the injured subjects (injured side minus healthy side) decreased from −11.8 ± 4.5 Ω when the injury was acute (within a month of the injury date) to −1.0 ± 4.0 Ω during recovery (four to seven months after corrective surgery). The difference in reactance decreased from 4.9 ± 2.6 Ω to 2.3 ± 2.0 Ω. Furthermore, the absolute difference in resistance between the knees decreased from 11.8 ± 4.6 Ω to 3.6 ± 1.7 Ω ($p<0.05$, two sample t-test with unknown and unequal variances).

The estimated probability density for the difference in resistance and difference reactance between the knees (left minus right) is also shown in Fig. 2(b). The probability density estimation was done using Gaussian kernel density estimation where the bandwidth is

Author Manuscript Author Manuscript Author Manuscript Author Manuscript

estimated using Scott's rule [22]. This kind of visualization helps show how the injured subjects' data points move toward where the healthy subjects' data points are denser, as recovery occurs.

The results seen for the knee resistances were consistent with expected physiological changes, as edema commonly accompanies injuries and local excess fluid accumulation results in lower tissue resistance. The injected current at 50 kHz flows through both extracellular and intracellular space [2], however, we cannot differentiate the contribution of either fluid space to the resistance change measured. Tissue resistance has also been argued to be proportional to new tissue growth and to fibrin clotting which are processes that occur during wound healing [11]. Therefore, as the edema decreases and injured tissue repair occurs during injury recovery, the injured knee's resistance increases and the absolute difference in resistance between the injured and healthy knees decreases.

Tissue reactance is related to cell membranes as they are made of lipid layers which have a capacitive effect. Negative reactance increases with cell mass and cell wall integrity which can both decrease (thus elevating reactance) due to injury [11]. Therefore, the observed knee's reduced reactance after injury is consistent with anticipated physiological changes as well. The results presented also agree with previous studies existing on assessing knee or lower limb health using bioimpedance [12–14, 23].

2) Day-to-Day Variability in EBI Measurements—The absolute difference in resistance and reactance between the left and the right knees are potential biomarkers for knee health monitoring as discussed in Section III.A.1. Knee bioimpedance measurements taken from five subjects in three different days (within a week) showed that the average day-to-day variability (standard deviation) of the absolute difference in knee resistances were 2.5Ω. The average day to day variability for the absolute difference in reactances was 1.2Ω.

3) Investigating Effects of Local Heating/Cooling on EBI—The results for the local tissue heating/cooling test are shown in Fig. 3. The mean knee resistance has been shown with error bars at 0 (baseline), 5, 10, 15 minutes into the heating/cooling for the seven subjects. Note that for each subject, the baseline knee resistance was subtracted from the measured resistance to show the deviation from the baseline. The difference between the baseline resistances for the subjects and the resistances measured at 5, 10 and 15 minutes was statistically significantly different than the baseline resistances ($p<0.01$) for both heating and cooling. A paired ttest was used to calculate the statistical significance as this test is effective in comparing dependent observations that have been obtained in pairs (the knee resistance measured at baseline temperature and that measured after a certain amount of heating/cooling) [24]. The skin temperature at the patella, at these time instances during heating were: 25.7±3.0 °C (baseline), 34.7±2.8 °C, 36.1±1.8 °C and 36.1±1.4 °C, respectively. The temperatures for cooling were: 25.6±1.3 °C (baseline), 19.5±2.7 °C, 18.3±3.1 °C and 18.0±3.3 °C, respectively. Though the temperature values are similar, for the third and fourth data points during heating and cooling respectively, these skin temperatures were held for an additional five minutes between the third and fourth data points; accordingly, the temperature within the tissue itself continued to increase (or decrease for cooling) throughout the measurement. The temperature data points also

Author Manuscript Author Manuscript Author Manuscript Author Manuscript

demonstrate that the heating or cooling rate of the patella, decreased with time, approaching zero towards the fourth data point.

Modulation of tissue temperature should cause changes in the local interstitial fluid volume. Heating will decrease the pre- to post-capillary resistance ratios causing net capillary filtration, while cooling will increase the pre- to post-capillary resistance ratio and thus cause net capillary absorption [21]. Fig. 3 demonstrates that our EBI measures were sufficiently sensitive to detect the small theoretical changes in interstitial fluid volume with local heating (increased interstitial fluid) and cooling (decreased interstitial fluid). It can be noted as the skin and underlying tissue progressively warmed or cooled, an expected progressive change in resistivity was observed. This demonstrates that the bioimpedance measurement system is sufficiently sensitive to detect small changes in interstitial fluid (edema) corresponding to a few Ohms change in tissue resistance.

These results also suggest that changes in knee temperature due to enviromental factors (e.g. hot or cold weather) or activity (e.g. exercise) is expected to effect EBI measurements. This suggests that a temperature sensor would be a good addition to a future wearable device for knee joint health monitoring. Such a sensor could be used to gate the EBI signals such that measurements are accepted, only when the knee temperature is within certain limits. This will allow the measurements taken in a wearable setting to be more consistent.

B. Towards a Wearable Sensor System: Position Identification and Dry Electrodes

1) Position Identification Algorithm—The resistance signal and the x-axis acceleration signal from the accelerometer on the shank ($a_{sh,x}(t)$) are shown on Fig. 4(b). The time intervals where the subject is in the correct position (seated, legs extended and supported) for the measurement to be acceptable are shown in red, while all others are shown in blue: subject standing, seated with legs bent 90°, seated leg crossed, walking). The dependence of the resistance signal on knee posture and the variability of the signal due to motion can be seen on this figure. It can also be seen that the mean value of $a_{sh,x}(t)$) within a given window can be a good indicator of the subject's knee posture, while the standard deviation of $a_{sh,x}(t)$ can be a good indicator of the presence of motion artifacts. Similar arguments can be made about the mean and standard deviations of the signals $a_{sh,y}(t)$, $a_{th,x}(t)$ and $a_{th,y}(t)$; justifying the use of these features in the position identification algorithm.

The LOSO cross-validated accuracy of the algorithm proposed in Section II.B and tested as described in Section II.C.4 was 97.4 ± 2.6%. The baseline misclassification rate (when the most probable class, reject (0), is always chosen) was 71.4%, and the accuracy achieved using the aforementioned algorithm was considerably higher. The LOSO cross-validated precision of the algorithm was 98.2 ± 2.8%. The standard deviation of the resistance signal without gating as discussed in Section II.C.4, averaged over all subjects was 3.3 ± 1.2Ω (range: 1.7Ω–5.5 Ω). With the application of the algorithm and gating, the averaged standard deviation dropped to 0.5 ± 0.3Ω (range: 0.2 Ω–1.2 Ω). The standard deviation of the reactance signal without gating, averaged over all subjects was 0.8 ± 0.5Ω (range: 0.4 Ω–1.2 Ω) and with gating it dropped to 0.2 ± 0.1Ω (range: 0.1 Ω–0.3 Ω). The signals obtained using gating were less variable due to consistent subject positioning.

Author Manuscript Author Manuscript Author Manuscript Author Manuscript

Consistent subject positioning in EBI measurements are critical in order to eliminate posture and motion related signal variability, which can blur the changes in the signals due to physiological effects. This consistency is established in the experiments in Sections II.C.1,2 and 3 by user guidance. The results presented in this section are a demonstration of how accelerometers can be used to automatically decide to take EBI measurements when the subject is in a certain position, eliminating the need for user guidance. An algorithm requiring a one-time offline training similar to this can be implemented on a smart phone that wirelessly communicates with the bioimpedance hardware, which is a step towards creating a “Smart Brace” monitoring knee impedance.

2) Evaluation of a Knee Wrap with Dry Electrodes Integrated—Another step towards the smart wrap for knee impedance monitoring is to test functionality with dry electrodes rather than wet electrodes. Wet Ag/AgCl electrodes are less suitable for a wearable system as they are disposable and need to be replaced frequently; dry electrodes on the other hand are more durable. However, dry electrodes are more challenging to use due to higher skin-electrode interface impedance and lack of an adhesive material (as found in wet Ag/AgCl electrodes) to fix the location of the electrode [25]. Increased contact area will reduce the skin electrode impedance [26].

The resistance measured using dry electrodes (R_{dry}) from seven subjects (14 knees), plotted against that measured using wet electrodes (R_{wet}) is shown on Fig. 5(d), along with the linear regression line and the 95% confidence interval for the regression. The r^2 score for the regression was 0.8. The corresponding plot for the reactance (X_{dry} versus X_{wet}) is shown in Fig. 5(e). The r^2 score for the corresponding regression was 0.9. These results indicate that the variations in the EBI measurements by wet electrodes can also reliably be measured using the dry versions within the designed knee brace.

The resistance measurements obtained using wet electrodes are larger than that obtained using dry electrodes. A similar argument is true for the measured negative reactance. This can be attributed to the phenomenon of current constriction [27]. The wet gel electrodes used have an electrode surface area of 2.08 inch^2 (1.6 inch by 1.3 inch), while the dry electrodes have a surface area of 9.60 inch^2 (five copper plates), 4.6 times larger than that of the wet electrodes. The smaller surface area of the wet electrodes constricts the path the injected current takes, causing a higher resistance to be measured compared to the resistance measured using the larger dry electrodes. A similar argument can be made for the measured reactance. The absolute difference in measurements between the dry and the wet electrodes can be compensated for by using a mapping between the wet and dry electrode measurements as shown in Fig. 5(d) and (e).

IV. Conclusions and Future Work

In this paper we describe a bioimpedance measurement system intended for wearable use, and demonstrate its ability to acquire physiologically relevant measurements from the knee joint. Human subject experiments were used to demonstrate how the knee impedance measured using the system provides information related to knee joint edema and injury, along with longitudinal changes during recovery. A validation study was conducted to show

Author Manuscript Author Manuscript Author Manuscript Author Manuscript

the ability of the measurement system in detecting small changes in interstitial fluid volume due to local tissue heating or cooling, demonstrating the sensitivity of the measurement system to small changes in interstitial fluid volume. A position detection algorithm and the usability of the system using dry copper electrodes was presented as a step towards reducing user guidance and making the system more feasible for a wearable setting.

Future efforts to develop a wearable system will focus on (a) hardware miniaturization and integration into a knee brace and including textile electrodes rather than copper ones; (b) applying this technology to other joints such as the shoulder; and (c) developing a system sufficiently robust for unilateral rather than bilateral use (i.e., without the need for comparing the left to right knee); (d) the integration of a temperature sensor to the system, to gate EBI signals, so that measurements are taken with consistent knee temperatures.

Acknowledgments

This material is based upon work supported in part by the Defense Advanced Research Projects Agency, Arlington, VA under Contract W911NF-14-C-0058, and in part by the National Institutes of Health, National Institute of Biomedical Imaging and Bioengineering, Grant 1R01EB023808, as part of the NSF/NIH Smart and Connected Health Program.

References

1. Ivorra A. Bioimpedance monitoring for physicians: an overview. Centre Nacional de Microelectrònica Biomedical Applications Group. 2003:11, 17.
2. Grimnes, S., Martinsen, O. Bioimpedance and Bioelectricity Basics. 2. Oxford, UK: Academic; 2008.
3. Kyle UG, et al. Bioelectrical impedance analysis—part I: review of principles and methods. Clinical Nutrition. Oct; 2004 23(5):1226–1243. [PubMed: 15380917]
4. Ulrich MM, et al. Body fluid volume determination via body composition spectroscopy in health and disease. Physiological Measurement. 2006; 27(9):921. [PubMed: 16868355]
5. Piccoli A, et al. A new method for monitoring body fluid variation by bioimpedance analysis: The RXc graph. Kidney International. Aug 1; 1994 46(2):534–539. [PubMed: 7967368]
6. Nyboer J, Kreider MM, Hannapel L. Electrical Impedance Plethysmography: A Physical and Physiologic Approach to Peripheral Vascular Study. Circulation. 1950; 2(6):811–821. [PubMed: 14783833]
7. Kubicek WG, Patterson RP, Witsoe DA. Impedance Cardiography as a Noninvasive Method of Monitoring Cardiac Function and Other Parameters of the Cardiovascular System. Annals of the New York Academy of Sciences. 1970; 170(2):724–732.
8. Miles DS, et al. Estimation of cardiac output by electrical impedance during arm exercise in women. Journal of Applied Physiology. 1981; 51(6):1488–1492. [PubMed: 7319881]
9. Zhang Y, et al. Cardiac Output Monitoring by Impedance Cardiography During Treadmill Exercise. IEEE Transactions on Biomedical Engineering. 1986; BME-33(11):1037–1042.
10. Sola J, et al. Chest Pulse-Wave Velocity: A Novel Approach to Assess Arterial Stiffness. IEEE Transactions on Biomedical Engineering. 2011; 58(1):215–223. [PubMed: 20813631]
11. Lukaski H, Moore M. Bioelectrical Impedance Assessment of Wound Healing. J Diabetes Sci Technol. 2012; 6(1):209–212. [PubMed: 22401341]
12. Nescolarde L, et al. Localized bioimpedance to assess muscle injury. Physiological Measurement. 2013; 34(2):237. [PubMed: 23354019]
13. Nescolarde L, et al. Effects of muscle injury severity on localized bioimpedance measurements. Physiological measurement. 2014; 36(1):27. [PubMed: 25500910]

Author Manuscript Author Manuscript Author Manuscript Author Manuscript

14. Pichonnaz C, et al. Bioimpedance spectroscopy for swelling evaluation following total knee arthroplasty: a validation study. BMC Musculoskeletal Disorders. 2015; 16(1):1–8. [PubMed: 25637090]
15. Hersek S, Toreyin H, Inan OT. A Robust System for Longitudinal Knee Joint Edema and Blood Flow Assessment Based on Vector Bioimpedance Measurements. IEEE Transactions on Biomedical Circuits and Systems. 2016; 10(3):545–555. [PubMed: 26841413]
16. Fabrizi L, et al. Analysis of resting noise characteristics of three EIT systems in order to compare suitability for time difference imaging with scalp electrodes during epileptic seizures. Physiological measurement. 2007; 28(7):S217. [PubMed: 17664637]
17. Choudhari PC, Panse M. Artifact Removal from the Radial Bioimpedance Signal using Adaptive Wavelet Packet Transform. International Journal of Computational Engineering Research (IJCER). Jul; 2014 4(7):2250–3005.
18. Medrano G, Leonhardt S, Zhang P. Modeling the influence of body position in bioimpedance measurements. :3934–3937.
19. Friedman, J., Hastie, T., Tibshirani, R. Springer series in statistics. Springer; Berlin: 2001. The elements of statistical learning; p. 417-426.
20. Raschka, S. Python Machine Learning. Packt Publishing Ltd; 2015. p. 210-213.
21. Sawka, MN. Body Fluid Responses and Hypohydration During Exercise-Heat Stress. In: Pandolf, KB.Sawka, MN., Gonzalez, RR., editors. Human Performance Physiology and Environmental Medicine at Terrestrial Extremes. Indianapolis, IN: Brown & Benchmark Press; 1988. p. 236-240.
22. Jones MC, Marron JS, Sheather SJ. A brief survey of bandwidth selection for density estimation. Journal of the American Statistical Association. 1996; 91(433):401–407.
23. Neves EB, et al. Knee bioelectric impedance assessment in healthy/with osteoarthritis subjects. Physiological measurement. 2009; 31(2):207. [PubMed: 20016115]
24. Hsu H, Lachenbruch PA. Paired t test. Wiley Encyclopedia of Clinical Trials. 2008
25. Chi YM, Jung TP, Cauwenberghs G. Dry-contact and noncontact biopotential electrodes: methodological review. Biomedical Engineering, IEEE Reviews in. 2010; 3:106–119.
26. Chen YH, et al. Soft, comfortable polymer dry electrodes for high quality ECG and EEG recording. Sensors. 2014; 14(12):23758–23780. [PubMed: 25513825]
27. Martinsen, OG., Grimnes, S. Bioimpedance and bioelectricity basics. Academic press; 2011. p. 169

Author Manuscript Author Manuscript Author Manuscript Author Manuscript

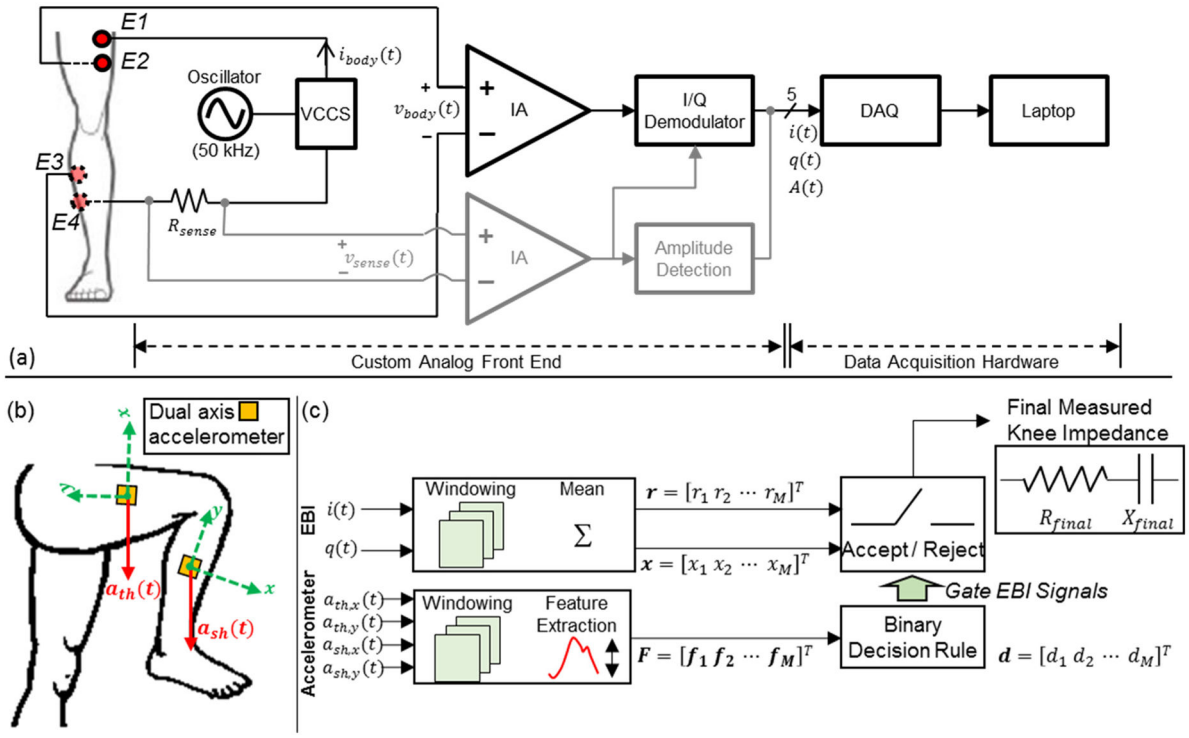

Fig. 1.

(a) A block diagram of the bioimpedance measurement system. E1–E4 represents the electrodes that interface to the body, where E1 and E4 are current electrodes, and E2 and E3 are voltage electrodes. The voltage signal across the resistor, R_{sense}, ($v_{sense}(t)$) is used to sense the injected current. The amplitude of this signal, $A(t)$, is detected and used to monitor the amplitude of the current ($i_{body}(t)$) passing through the knee joint. The voltage signal $v_{body}(t)$ is inphase/quadrature (I/Q) demodulated to acquire the signals $i(t)$ and $q(t)$ which relate to the resistance and reactance of the measured segment. VCCS: voltage controlled current source, DAQ: data acquisition system, IA: instrumentation amplifier. (b) Dual axis accelerometers were place on the thigh and the shank to gate the EBI signals. The acceleration signals acquired from the thigh are $\boldsymbol{a_{th}(t)} = [a_{th,x}(t)\ a_{th,y}(t)]^T$ and those acquired from the shank are $\boldsymbol{a_{sh}(t)} = [a_{sh,x}(t)\ a_{sh,y}(t)]^T$. (c) Algorithm for identifying the time intervals when the user is in the optimal position to acquire measurements (sitting, legs extended and supported). The acceptable time intervals are identified by extracting features from the dual axis accelerometer signals ($a_{th,x}(t)$, $a_{th,y}(t)$, $a_{sh,x}(t)$, $a_{sh,y}(t)$) and using these features to make a decision. The binary decision rule is trained once before-hand. The accepted time intervals are used to obtain the knee resistance (R_{final}) and reactance (X_{final}) using the voltage signals $i(t)$ and $q(t)$.

Author Manuscript Author Manuscript Author Manuscript Author Manuscript

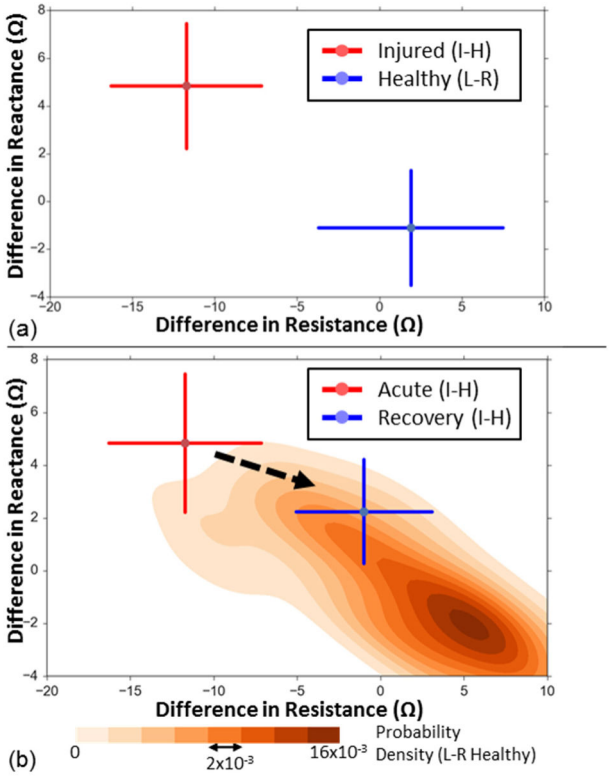

Fig. 2.

(a) The difference in resistance versus the difference in reactance for the healthy and injured subjects. For the healthy subjects (shown in blue, N=42), the difference is that between the left and the right knee (L–R) and for the injured subjects (shown in red, N=7) it is that between the injured and the healthy knee (I–H). The error bars indicate one standard deviation. (b) The difference in resistance versus the difference in reactance for the injured subjects (N=7), when the injury is acute (within one month of the measurement take, shown in red) and during recovery (four to seven months after corrective surgery, in blue). For these subjects, the difference shown is I–H. The probability density of the healthy subjects' data (N=42, L–R difference), estimated using 2-dimensional Gaussian kernel density estimation is also visualized in shades of orange for comparison. The error bars indicate one standard deviation.

Author Manuscript Author Manuscript Author Manuscript Author Manuscript

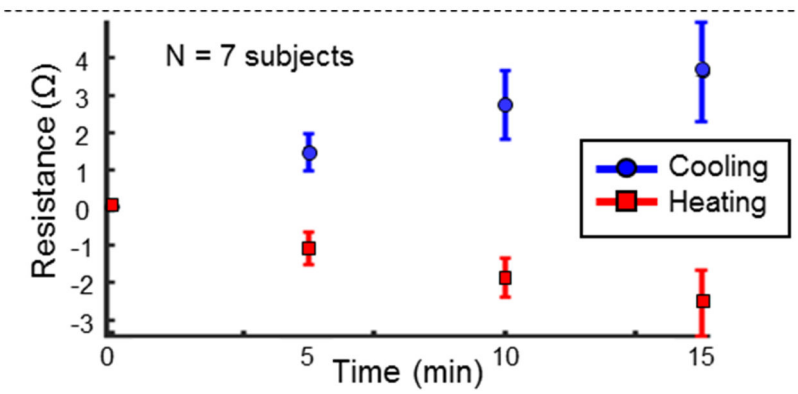

Fig. 3.

Mean knee resistances for seven subjects during heating (in red) and cooling (in blue) along with the standard deviations (shown in error bars). Note that each subject's baseline knee resistance (at time=0 minutes) was subtracted from the rest of their measurements to emphasize the change in knee resistance with heating/cooling. The data points shown are at 0,5,10 and 15 minutes into heating/cooling. The skin temperature at the patella, at these time instances during heating were: 25.7±3.0 °C, 34.7±2.8 °C, 36.1±1.8 °C and 36.1±1.4 °C. The temperatures for cooling were: 25.6±1.3 °C, 19.5±2.7 °C, 18.3±3.1 °C and 18.0±3.3 °C.

Author Manuscript Author Manuscript Author Manuscript Author Manuscript

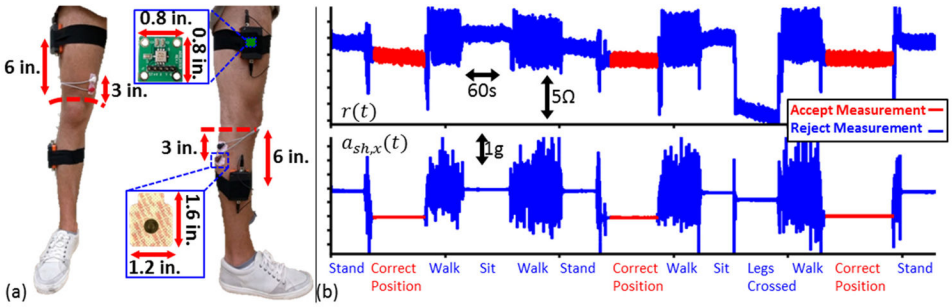

Fig. 4.

(a) Electrode positioning using wet Ag/AgCl electrodes as well as the positioning used for the two dual axis accelerometers. (b) The resistance ($r(t)$) signal and the x-axis shank acceleration signal ($a_{sh,x}(t)$) measured from a subject during various activities. The time intervals marked in red are when the subject is in the correct position for taking measurements (sitting, legs extended and supported). The measurements taken when the subject is in the correct position are to be accepted, all other measurements (shown in blue) should be rejected.

Author Manuscript Author Manuscript Author Manuscript Author Manuscript

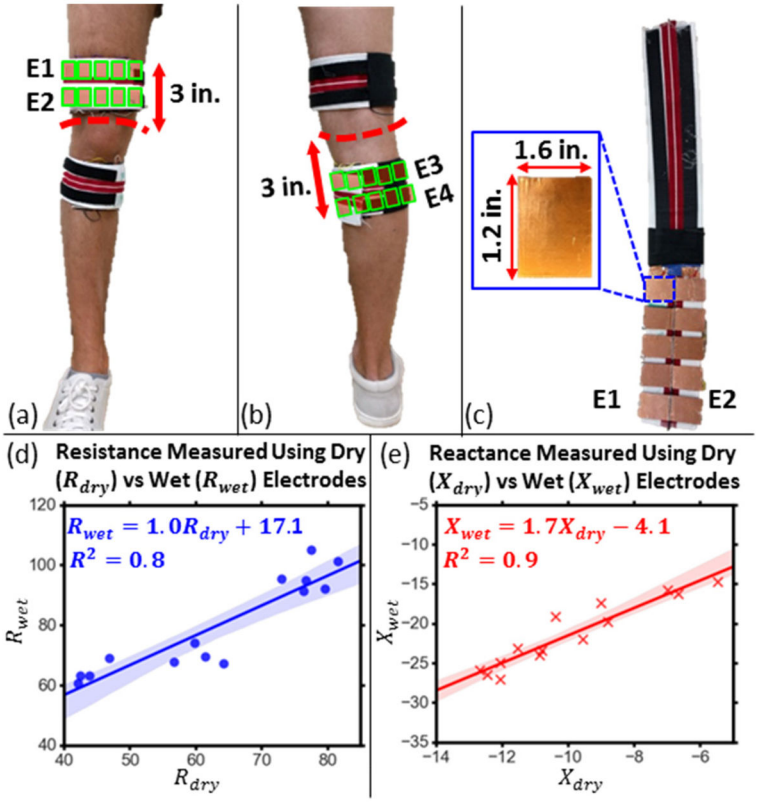

Fig. 5.

(a),(b) Electrode placement for the knee wrap with integrated dry copper electrodes. The electrode positions inside the wrap are indicated using green rectangles. (c) Dry, copper electrodes integrated into a knee wrap. Each electrode is made of five 1.6 inch by 1.2 inch rectangles cut out of plastic, covered with copper tape. (d) Resistance measured using dry electrodes (R_{dyr}) versus that measured using wet electrodes (R_{wet}) along with the linear regression line and the 95% confidence interval for the regression shaded. (e) Reactance measured using dry electrodes (X_{dyr}) versus that measured using wet electrodes (X_{wet}) along with the linear regression line and the 95% confidence interval for the regression shaded.